



Research Article

Energy and exergy analysis of a combined system: cascade organic Rankine cycle and cascade refrigeration cycle

Touaibi RABAH^{1,*}, Hasan KOTEN², Boudjema FADHILA¹, Selmane SALMA¹,
Hemis MOHAMED¹

¹Faculty of Science and Technology, Djilali Bounaama University, Ain Defla, Algeria

²Istanbul Medeniyet University, Mechanical Engineering Department, Istanbul, Turkey

ARTICLE INFO

Article history

Received: 03 October 2019

Accepted: 08 January 2020

Key words:

Organic rankine cycle; Cascade refrigeration; Exergy analysis

ABSTRACT

In this paper, a new combined system is proposed for recovering thermal energy at medium temperature using a cascade organic Rankine cycle to feed a cascade refrigeration cycle. Energy and exergy analysis is applied to the combined system to determine its performance using different working fluids under the same operating conditions taking into account the effect of some operating parameters and the selection of organic fluids on cycle performance. The pair of organic fluid (Toluene/R245fa) used for the cascade organic Rankine cycle and the pairs (R717/R744, R717/R23, R134a/R23) used for the cascade refrigeration cycles. The results show that the combined system function with the couple (R717/R23) for cascade refrigeration cycle gives better exergy efficiency 50.03% compared to other couples, 49.57% for the couple (R717/R744), and 48.01% for the couple (R134a/R23). The thermodynamic evaluation shows that the operating temperatures, such as the cascade organic Rankine cycle evaporation temperature and the cascade refrigeration cycle evaporation temperature influence the performance of the combined system.

Cite this article as: Rabah T, Kote H, Fadhila B, Salma S, Mohamed H. Energy and exergy analysis of a combined system: cascade organic Rankine cycle and cascade refrigeration cycle. J Ther Eng 2021;7(5):1139–1149.

INTRODUCTION

Industrial processes are generally characterized by the loss of energy in a form of heat. This dissipated energy not only reduces the effectiveness of these processes but also contributes to the environmental impacts associated with

the use of the fossil fuel. These low-temperature discharges cannot be used to generate electricity via a steam thermal plant (Conventional Rankine Cycle). Alternative technologies like the organic Rankine Cycle (ORC) can convert the waste heat to electricity at a relatively low temperature.

*Corresponding author.

*E-mail address: ra.touaibi@gmail.com

This paper was recommended for publication in revised form by Regional Editor Jovana Radulovic



Hence, they contribute significantly to reduce fuel costs and pollution as well.

Organic Rankine cycles are cycles of mechanical power generated from waste heat. The organic Rankine Cycles are variants of water vapour cycles, but they use the heat sources to produce mechanical energy at low or medium temperatures [1, 2]. Bellos and Tzivanidis optimized a system with Organic Rankine Cycle (ORC), an absorption chiller for cooling, heating, and electricity production. They found the maximum exergy efficiency to be 29.42% with toluene [3]. Furthermore, Bellos and Tzivanidis [4] examined a trigeneration system including a generator, an ejector, a condenser, a turbine, and an evaporator where the studied configuration forms a system able to produce heating, cooling, and electricity. The heat source generally comes from geothermal energy [5–8], biomass energy [9, 10], or industrial waste streams [11, 12], otherwise solar energy [13, 14].

The energy and exergy analysis of a combined cycle including a vapour-cooled refrigeration cycle and an organic Rankine cycle has been studied by [15–20]. Another system for cold production using the absorption machine has been studied by [21–25]. Cooling technologies operating at low temperatures have attracted the attention of many researchers in different contexts. A study was carried out by Lee et al. [26] on thermodynamic analysis of a cascade refrigeration system using carbon dioxide (CO_2) and ammonia (NH_3) as refrigerants. Regarding the same topic area, Getu et al. [27] conducted their study on the system (R744/R717) for optimizing the design and parameters of the studied system. The analysis here is based on sub-cooling at the condenser outlet at 40°C and overheating at the evaporator outlet with 50°C to develop mathematical expressions for the maximum COP. The results revealed that COP max was highest for ethanol followed by R717 and it was lower for R404 under the same conditions. Kilicarslan et al. [28] studied an irreversibility analysis of a cascade refrigeration system for various refrigerant couples, namely R152a/R23, R290/R23, R507/R23, R234a/R23, R717/R23, and R404a/R23; the degrees of the condenser sub-cooling and evaporator superheat are 5°C and 7°C for all cases.

They found that COP of the cascade refrigeration system increases and the irreversibility decreases with rising evaporator temperature and polytrophic efficiency for all studied refrigerant couples and vice versa for the increasing of the condenser temperature. Dapazo et al. [29] have performed an analysis of CO_2/NH_3 cascade cooling system design and its operating parameters and how they influence the COP and the exergy efficiency of that system; they concluded that the COP increases by 70% when the evaporation temperature of CO_2 varies from –55°C to –30°C and hence other parameters influence on the COP increases as well, but when the condenser temperature of NH_3 increases from 25°C to 50°C, the COP decreases. The

authors tried also to use NH_3 and CO_2 as refrigerants to provide a cooling capacity at an evaporating temperature of –50°C [30]. This refrigeration capacity was showed in the results to be 9.45 kW. A thermodynamic analysis of theoretical performance for a cascade refrigeration system was conducted by Yst and Karakurt [31]; Different refrigerant couples are used in which the pair R23/R717 showed the best performances compared to the other pairs of refrigerants. The rate of total exergy destruction decreases with the increase of the temperature of the evaporator and increases with the increase of the temperature of the condenser. For the efficient recovery of waste heat in marine applications, a dual Organic Rankine Cycle system in parallel was proposed by Yun et al. [32]. The results showed that when the total annual output power in double ORC configuration ranges from 103% to 115%, the double ORC produces more energy than the single ORC. Molès et al. [33] studied a thermodynamic analysis of the performance of a combined system of organic Rankine cycle and vapour compression cycle driven by heat sources at low temperature and using low GWP fluids. The thermal COP of the ORC-VCC system varied between 0.30 and 1.10; it was concluded that the thermal COP increased with the ORC and VCC evaporating temperatures and decreased with the condensing temperature.

A new cascade cycle to recover energy from a medium-temperature waste stream was proposed by Sadreddini et al. [34] where both energy and exergy analyses are applied to the system. The results showed that the best performance is for a cascade cycle with Pentane as a working fluid for the ORC section. A combined system using a single ORC cycle stage to power a cascade refrigeration system has been studied by Lizarte et al. [35]. In the present study, a new configuration for a cascade refrigeration system is used; this configuration uses a two-stage cascaded ORC cycle instead of a single-stage, it is noted that each stage of the ORC cycle supply one stage of the cascade refrigeration cycle, knowing also that the upper stage turbine of the ORC cycle supply the compressor of the upper stage of the refrigeration cycle and the turbine of the lower stage of the ORC cycle supplies the compressor of the low stage of the refrigeration cycle. In addition, several pairs of organic fluids were used to conduct a comparative study in order to select the best pair that gives good performance to the combined system. The pair of the organics fluids used for each cycle are: (toluene / R245fa) chosen to supply the ORC cycle in cascade and the pairs (R717 / R744, R717 / R23, R134a / R23) chosen for the refrigeration cycle CRS Cascade.

The aim of this study is to improve the system performance. In addition, a comparative study of different couples of organic fluids was followed to select the best couple that can give good energy efficiency. The pairs used in this study are (Toluene/R245fa), (R717/R744, R717/R23, R134a/R23) for the cascade ORC and the cascade CRS cycles, respectively.

DESCRIPTION OF THE COMBINED SYSTEM (ORC-CRS)

The combined system consists of two main cycles: a cascade Rankine organic cycle used for mechanical energy production and a cascade refrigeration cycle used for refrigeration. The mechanical power generated by the ORC cycle turbines is transmitted to the compressors to supply them with energy and so to complete the refrigeration process.

THERMODYNAMIC ANALYSIS

In this section, a thermodynamic modelling study is presented and the mass balance is defined as follows [36, 37];

$$\sum \dot{m}_{in} = \sum \dot{m}_{out} \quad (1)$$

Where m , is the mass flow rate (kg/s),

According to first law of thermodynamics, the energy balance equation is:

$$\sum \dot{m}_{in} h_{in} + \sum \dot{Q}_{in} + \sum \dot{W}_{in} = \sum \dot{m}_{out} h_{out} + \sum \dot{Q}_{out} + \sum \dot{W}_{out} \quad (2)$$

Where; \dot{Q} , \dot{W} and h are the heat transfer rate, work rate and specific enthalpy. The entropy balance equality can be described as follows:

$$\sum \dot{m}_{in} s_{in} + \sum \left(\frac{\dot{Q}}{T} \right)_{in} + \dot{s}_{gen} = \sum \dot{m}_{out} s_{out} + \sum \left(\frac{\dot{Q}}{T} \right)_{out} \quad (3)$$

Where s and \dot{S} are the specific entropy and entropy generation rate, respectively. Based on the second law of thermodynamic analysis, the exergy equity defined as given below;

$$\sum \dot{m}_{in} ex_{in} + \sum \dot{E}x_{in}^Q + \sum \dot{E}x_{in}^W = \sum \dot{m}_{out} ex_{out} + \sum \dot{E}x_{out}^Q + \sum \dot{E}x_{out}^W + \dot{E}x_D \quad (4)$$

The exergy destruction denoted by $\dot{E}x_D$ and the other terms in Eq. (4) can be given as:

$$\dot{E}x_D = T_0 \dot{S}_{gen} \quad (5)$$

$$\dot{E}x_Q = \left(1 - \frac{T_0}{T} \right) \dot{Q} \quad (6)$$

$$\dot{E}x_W = \dot{W} \quad (7)$$

The flow exergy is inscribed as

$$ex_{ph} = h - h_0 - T_0(s - s_0) \quad (8)$$

The energy and exergy analysis of the ORC-CRS combined cycle requires the application of the first and second law of thermodynamics. The general equations corresponding to this principle are presented below (Table 1):

Performance Evaluation

The performance of the ORC-CRS combined system is determined by the following equations:

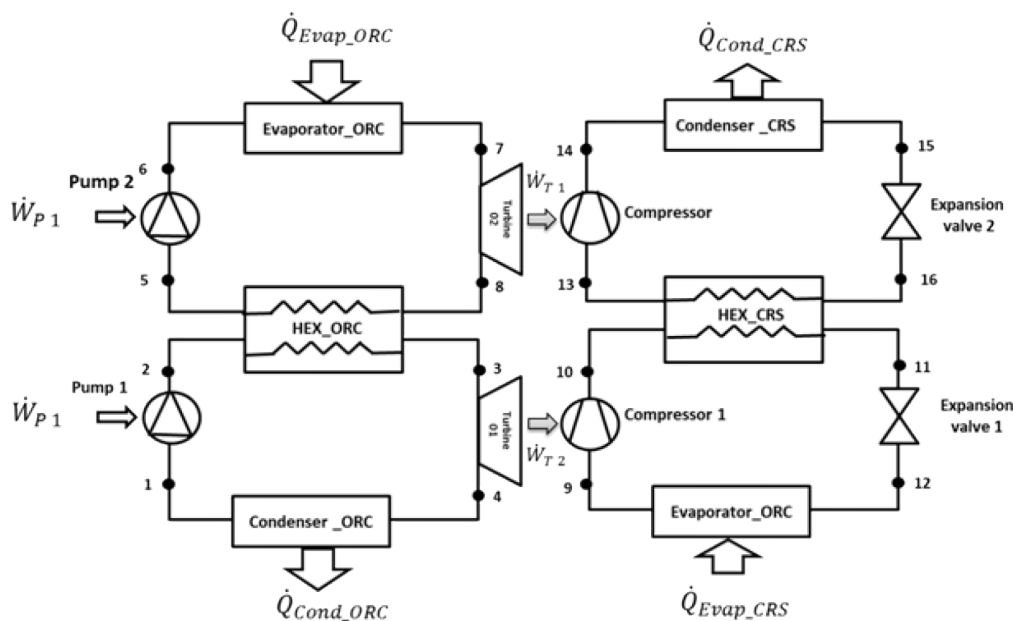


Figure 1. Schematic diagram of ORC-CRS combined system.

Table 1. Energy and exergy balance of combined cycle ORC-CRS

Components	Energy balance equations	Exergy balance equations
Pump 1	$\dot{m}_1 h_1 + \dot{W}_{P1} = \dot{m}_2 h_2$	$\dot{m}_1 ex_1 + \dot{W}_{P1} = \dot{m}_2 ex_2 + \dot{E}_{x,D,P1}$
Heat Exchanger ORC	$\dot{m}_2 h_2 + \dot{m}_8 h_8 = \dot{m}_3 h_3 + \dot{m}_5 h_5 + \dot{Q}_{L,ORC}^{HEX}$	$\dot{m}_2 ex_2 + \dot{m}_8 ex_8 = \dot{m}_3 ex_3 + \dot{m}_5 ex_5 + \dot{E}_{x,L,ORC}^{Q,HEX} + \dot{E}_{x,D,HEX,ORC}$
Turbine 1	$\dot{m}_3 h_3 = \dot{m}_4 h_4 = \dot{W}_{T1}$	$\dot{m}_3 ex_3 = \dot{m}_4 ex_4 = \dot{W}_{T1} + \dot{E}_{x,D,T1}$
Condenser ORC	$\dot{m}_4 h_4 = \dot{m}_1 h_1 = \dot{Q}_{Cond,ORC}$	$\dot{m}_4 ex_4 = \dot{m}_1 ex_1 + \dot{E}_{x,Cond,ORC}^{Q} = \dot{E}_{x,D,Cond,ORC}$
Pump 2	$\dot{m}_5 h_5 + \dot{W}_{P2} = \dot{m}_6 h_6$	$\dot{m}_5 ex_5 + \dot{W}_{P2} = \dot{m}_6 ex_6 + \dot{E}_{x,D,T2}$
Evaporator ORC	$\dot{m}_6 h_6 + \dot{Q}_{Evap,ORC} = \dot{m}_7 h_7$	$\dot{m}_6 ex_6 + \dot{E}_{Evap,ORC}^{Q} = \dot{m}_7 ex_7 + \dot{E}_{x,D,Evap,ORC}$
Turbine 2	$\dot{m}_7 h_7 = \dot{m}_8 h_8 + \dot{W}_{T2}$	$\dot{m}_7 ex_7 = \dot{m}_8 ex_8 + \dot{W}_{T2} + \dot{E}_{x,D,T2}$
Compressor 1	$\dot{m}_9 h_9 + \dot{W}_{C1} = \dot{m}_{10} h_{10}$	$\dot{m}_9 ex_9 + \dot{W}_{C1} = \dot{m}_{10} ex_{10} + \dot{E}_{x,D,C1}$
Heat Exchanger CRS	$\dot{m}_{10} h_{10} + \dot{m}_{16} h_{16} = \dot{m}_{11} h_{11} + \dot{m}_{13} h_{13} + \dot{Q}_{L,CRS}^{HEX}$	$\dot{m}_{10} ex_{10} + \dot{m}_{16} ex_{16} = \dot{m}_{11} ex_{11} + \dot{m}_{13} ex_{13} + \dot{E}_{x,L,CRS}^{Q,HEX} + \dot{E}_{x,D,HEX,CRS}$
Expansion valve 1	$\dot{m}_{11} h_{11} = \dot{m}_{12} h_{12}$	$\dot{m}_{11} ex_{11} = \dot{m}_{12} ex_{12} + \dot{E}_{x,D,Ev1}$
Evaporator CRS	$\dot{m}_{12} h_{12} + \dot{Q}_{Evap,CRS} = \dot{m}_9 h_9$	$\dot{m}_{12} ex_{12} + \dot{E}_{Evap,CRS}^{Q} = \dot{m}_9 ex_9 + \dot{E}_{x,D,Evap,CRS}$
Compressor 2	$\dot{m}_{13} h_{13} + \dot{W}_{C2} = \dot{m}_{14} h_{14}$	$\dot{m}_{13} ex_{13} + \dot{W}_{C2} = \dot{m}_{14} ex_{14} + \dot{E}_{x,D,C2}$
Condenser CRS	$\dot{m}_{14} h_{14} = \dot{m}_{16} h_{16} + \dot{Q}_{Cond,CRS}$	$\dot{m}_{14} ex_{14} = \dot{m}_{16} ex_{16} + \dot{E}_{x,Cond,CRS}^{Q} = \dot{E}_{x,D,Cond,CRS}$
Expansion valve 2	$\dot{m}_{15} h_{15} = \dot{m}_{16} h_{16}$	$\dot{m}_{15} ex_{15} = \dot{m}_{16} ex_{16} + \dot{E}_{x,D,Ev2}$
mass balance		
ORC Cycle: $\dot{m}_1 = \dot{m}_2 = \dot{m}_3 = \dot{m}_4 = \dot{m}_{L,ORC}$; $\dot{m}_5 = \dot{m}_6 = \dot{m}_7 = \dot{m}_8 = \dot{m}_{H,ORC}$		
CRS Cycle: $\dot{m}_9 = \dot{m}_{10} = \dot{m}_{11} = \dot{m}_{12} = \dot{m}_{L,CRS}$; $\dot{m}_{13} = \dot{m}_{14} = \dot{m}_{15} = \dot{m}_{16} = \dot{m}_{H,CRS}$		

The net mechanical power is:

$$\dot{W}_{net} = \dot{W}_T - \dot{W}_P \quad (9)$$

Thermal efficiency is written as:

$$\eta_{th,ORC} = \frac{\dot{W}_{net}}{\dot{Q}_{Evap,ORC}} \quad (10)$$

The coefficient of performance is presented as:

$$COP_{CRS} = \frac{Q_{Evap,CRS}}{\dot{W}_C} \quad (11)$$

The efficiency of the ORC-CRS system is:

$$\eta_{Ex,sys} = \eta_{Ex,ORC} \cdot \eta_{Ex,CRS} \quad (12)$$

The coefficient of performance of ORC-CRS system is written as:

$$COP_{sys} = \eta_{th,ORC} \cdot COP_{CRS} \quad (13)$$

RESULTS AND DISCUSSION

In this study, a novel design of the ORC-CRS combined system is based on a thermodynamic analysis. In this section, the effect of the operating parameters on the

performance of the combined system will be detailed. In each case, a couple of working fluids (Toluene/R245fa) is used for the cascade ORC cycle with R717/R23 as working fluid for the cascaded CRS cycle taking into account the fact that the thermodynamic properties are determined using Solkane and Coolpack software and that $\dot{W}_{net,ORC} = \dot{W}_{Com,CRS}$. Table 2 shows the input parameters values for the ORC-CRS combined system.

Before starting the parametric study on the ORC-CRS combined system, a comparative study based on the three couples organic fluids used for the CRS cascade refrigeration cycle is done. The findings are presented in Table 3 as follows:

Following the results obtained by the comparative study of the different pairs of organic fluids used by the CRS refrigeration cycle. The couple (R717/R23) gives a good exergy efficiency with a value of 50.03%. The thermodynamic characteristics of each point constituting the combined cycle (Table 4) have been first determined followed by the energetic and exergy performances of this system (Table 5).

Distribution of Exergy Destroyed in the ORC-CRS Combined System

The distribution of the destroyed exergy in the ORC-CRS combined system using the best organic fluid pair (Toluene/R245fa to cascade ORC cycle and R717/R23 to cascade CRS cycle) is studied. The results of Figure 2 shows

Table 2. Input parameters values of combined cycle

Parameters	Values	References
Mass flow rate of High ORC cycle, \dot{m}_{H_ORC} (kg/s)	1	This work
High Evaporator ORC Temperature, $T_{Evap_High_ORC}$ (°C)	310	This work
High Condenser ORC Temperature, $T_{Cond_High_ORC}$ (°C)	120	This work
Low Evaporator ORC Temperature, $T_{Evap_Low_ORC}$ (°C)	100	[15]
Low Condenser ORC Temperature, $T_{Cond_Low_ORC}$ (°C)	40	[15]
High Condenser CRS Temperature, $T_{Cond_High_CRS}$ (°C)	40	[20, 22]
High Evaporator CRS Temperature, $T_{Evap_High_CRS}$ (°C)	-10	[20, 22]
Low Condenser CRS Temperature, $T_{Cond_Low_CRS}$ (°C)	-12	[20, 22]
Low Evaporator CRS Temperature, $T_{Evap_Low_CRS}$ (°C)	-40	[20, 22]

Table 3. Results of comparative study based on the three couples organic fluids

	Organic fluids	$\eta_{Ex_ORS_CRS}$
Combined cycle	(Toluene/R245fa),(R134a/R23)	48.01%
ORC-CRS	(Toluene/R245fa),(R717/R744)	49.57%
	(Toluene/R245fa),(R717/R23)	50.03%

Table 4. Thermodynamic characteristics of the points of the combined cycle

State N°	Fluid type	T (C°)	P (bar)	h (kJ/kg)	s (kJ/kg)
1	R245fa	40	2.50	252.57	1.179
2	R245fa	40.57	12.64	253.35	1.179
3	R245fa	100	12.64	474.26	1.7912
4	R245fa	50.69	2.50	444.46	1.7912
5	Toluene	120	1.31	19.025	0.04887
6	Toluene	122.25	37.11	23.642	0.04887
7	Toluene	310	37.11	601.24	1.1934
8	Toluene	183.02	1.31	476.62	1.1934
9	R23	-40	7.09	337.91	1.6185
10	R23	9.75	18.85	362.6	1.6185
11	R23	-12	18.85	182.54	0.9368
12	R23	-40	7.09	182.54	0.9498
13	R717	-10	2.67	1446.84	5.78
14	R717	54.94	15.54	1707.74	5.78
15	R717	40	15.54	386.43	1.6303
16	R717	-10	2.679	386.43	1.7186

the largest exergy destroyed is in the ORC condenser by 62% and at the ORC exchanger by 13%.

Following the comparative study, a parametric study on the best organic fluid R717/R23 has been done. Latter is based on the effect of the operating temperatures; in particular, the evaporation temperature T_{Evap_ORC} and the evaporation temperature T_{Evap_CRS} on the exergy efficiency of the ORC-CRS combined cycle was carried out. In this part, the effect of ORC evaporation temperature on the performance of the CRS-ORC combined cycle was studied. For this, some operating parameters are fixed such as the evaporation temperature and the condensation temperature of the ORC and CRS cycle: $T_{Evap_CRS} = -40^\circ\text{C}$, $T_{cond_CRS} = 40^\circ\text{C}$, and . In addition, the evaporation temperature of the ORC varies between 200°C and 310°C.

Figures 3–5 shows the influence of ORC evaporation temperature on the coefficient of performance, the energy efficiency, and exergy efficiency of the ORC-CRS combined system, respectively. The other parameters are kept constant, which are presented in Table 2. Figure 3 shows the effect of the ORC evaporation temperature on the coefficient of performance of the combined system ORC-CRS. The result show that the coefficient of performance of system decreases considerably with the increase of the ORC evaporation temperature. The coefficient of performance decreased from 0.71 at a temperature of 200°C to a minimum value of 0.64 at the temperature of 310°C. Figure 4 shows the effect of the ORC evaporation temperature on the energy efficiency system of the ORC-CRS combined system. The results show that the energy efficiency of the combined system decreases considerably

Table 5. Performances of combined cycle: cascade ORC (Toluene / R245fa) and cascade CRS (R717 / R23):

Component	Power and heat transfer rate (kW)	Exergy destruction rate (kW)
Cycle ORC		
Pump 1	1.61	0
Pump 2	4.61	0
Turbine 1	61.66	0
Turbine 2	124.62	0
Condenser	397.23	213.57
Evaporator	577.59	46.14
Heat exchanger	457.59	37.13
\dot{m}_{H_ORC} (kg/s)	1	
\dot{m}_{L_ORC} (kg/s)	2.07	
\dot{W}_{net_ORC} (kW)	180.04	
η_{TH_ORC} (%)	31.17	
η_{EX_ORC} (%)	67.3	
Cycle CRS		
Compressor 1	60.04	0
Compressor 2	120	0
Condenser	607.8	9.89
Evaporator	377.54	1.36
Heat exchanger	487.78	13.26
expansion valve 1	–	9.47
expansion valve 2	–	12.18
\dot{m}_{H_CRS}	0.46	
\dot{m}_{L_CRS}	2.43	
COP_{CRS} (–)	2.09	
COP_{EX_CRS} (%)	0.74	
Combined cycle ORC-CRS		
$\eta_{sys} = 64.15\%$		$\eta_{EX} = 50.03\%$

reaches a maximum value of 70.95% at the temperature of 200°C and a minimum value of 64.66% at the temperature of 310°C.

On the other hand, the results of Figure 5 show that the exergy efficiency of the combined system decreases significantly with the increase of the ORC evaporation temperature from the maximum value of 69.55% to 50.03% over the temperature range of 200°C at 310°C.

The effect of the CRS evaporation temperature on the performances of the cascade refrigeration cycle and on the ORC-CRS combined cycle has been also studied in which the best selected organic fluid is used. To do this, some parameters are set; the evaporation temperature and the condensation temperature of the ORC cycle, as well as the condensation temperature of the CRS cycle, which respectively carry these values. $T_{Evap_ORC} = 310^\circ\text{C}$, $T_{Cond_ORC} = 40^\circ\text{C}$ and $T_{Cond_CRS} = 40^\circ\text{C}$, while the evaporation temperature varies over a temperature range from -60°C à -30°C . Figures 6–8 show the influence of CRS evaporation temperature on the coefficient of performance, the energy efficiency, and exergy efficiency of the ORC-CRS combined system, respectively while keeping the other parameters constant are presented in Table 2. The results of Figure 6 show that the coefficient of performance of the combined system increases considerably over the temperature range considered and reaches a maximum value of 1.05 at -30°C and the minimum value is 0.32 at -60°C . The results of Figure 7 show that the energy efficiency of the combined system increases considerably over the temperature range considered and reaches a maximum value of 75.15% at -30°C and the minimum value is 32.36 % at -60°C of temperature.

The results of Figure 8 show that the exergy efficiency of the combined system increases significantly with the increase of the CRS refrigeration temperature, the maximum value being 63.62% at -30°C and the minimum value of 38.11% at -60°C .

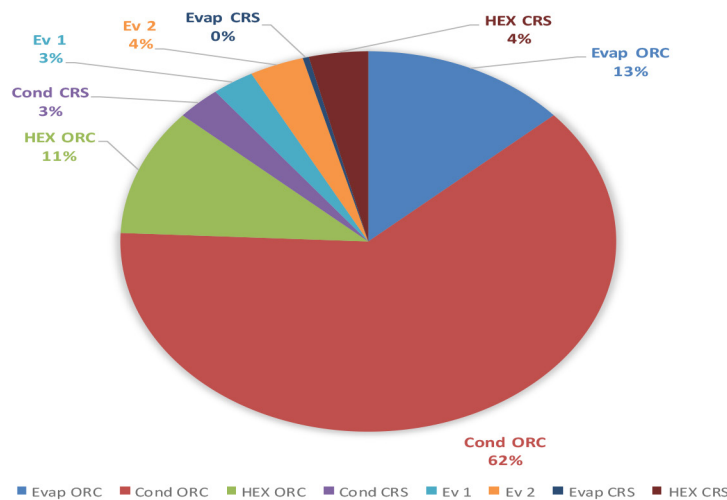


Figure 2. Distribution of exergy destroyed in the ORC-CRS combined system.

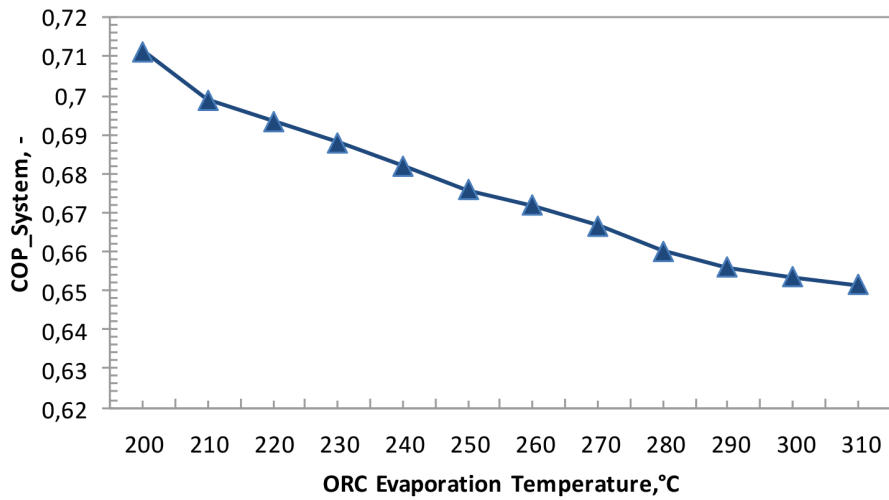


Figure 3. Effect of ORC evaporation temperature on coefficient of performance of system.

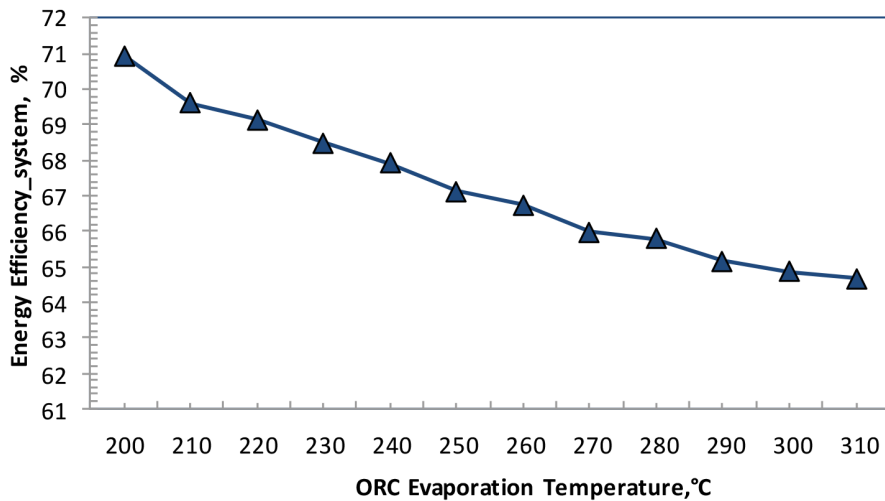


Figure 4. Effect of ORC evaporation temperature on energy efficiency of system.

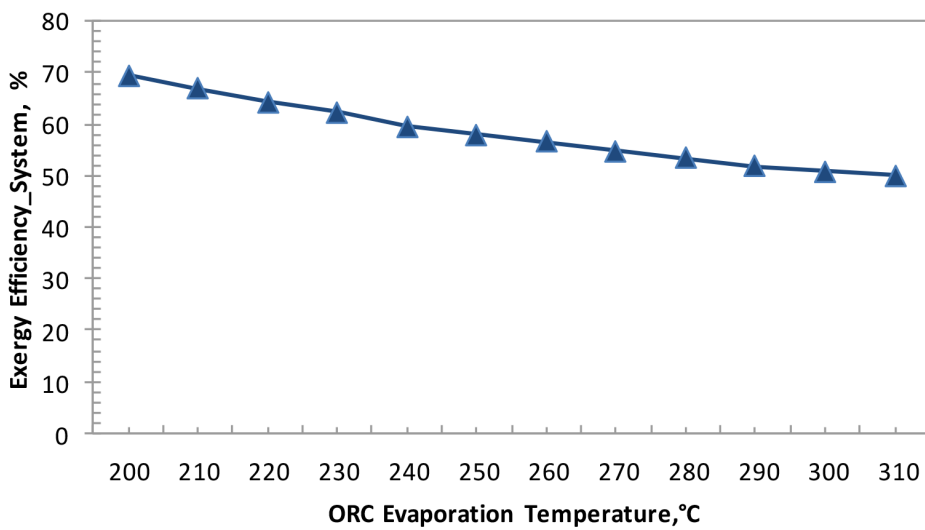


Figure 5. Effect of ORC evaporation temperature on exergy efficiency of system.

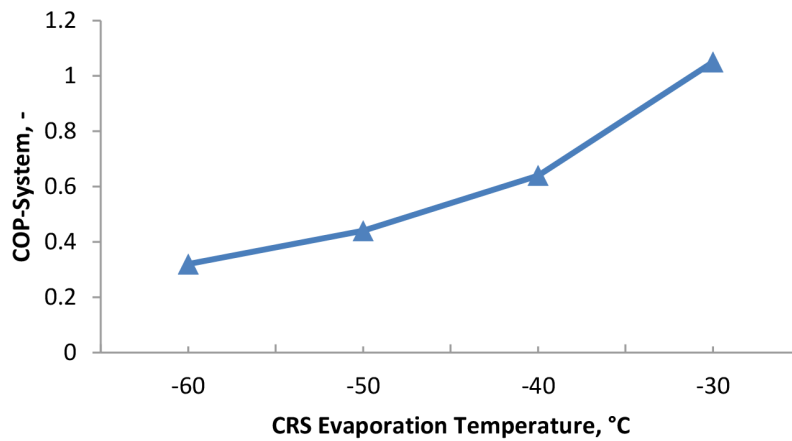


Figure 6. Effect of ORC evaporation temperature on exergy efficiency of system.

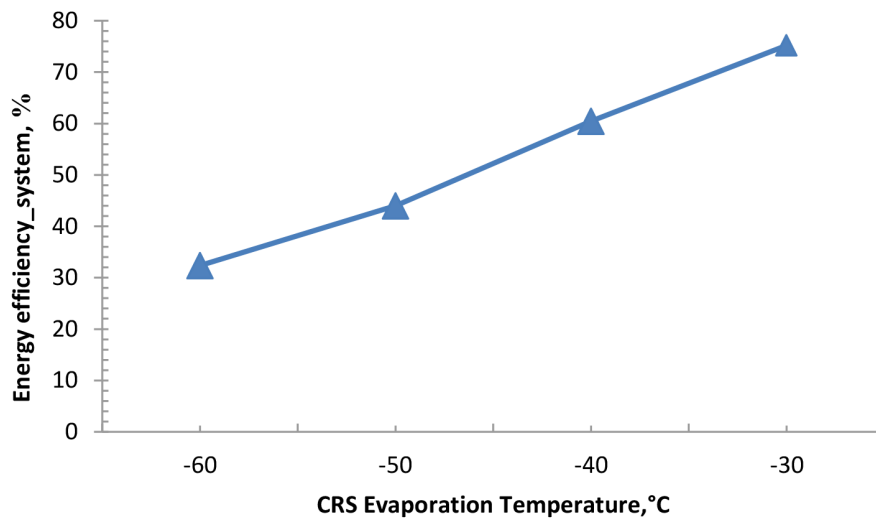


Figure 7. Effect of CRS evaporation temperature on energy efficiency of system.

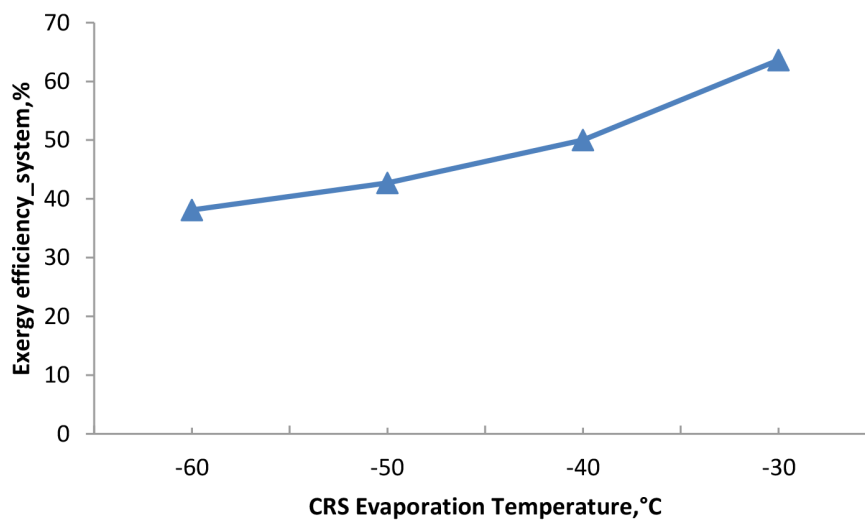


Figure 8. Effect of CRS evaporation temperature on exergy efficiency of system.

CONCLUSION

In order to improve the performance of a cascade refrigeration system (CRS), a new combined ORC / CRS system was used in this study where the energy produced by the ORC cycle has been used to supply mechanical compressors of the CRS cycle. From the results found, it was concluded that:

- The pair of R717/R23 gives better performances in terms of exergy efficiency for the CRS cycle with the Toluene / R245fa pair for the ORC cycle in cascade with 50% of , and the most great exergy destroyed was in the ORC condenser with 62%.
- The coefficient of performance of the system decreases considerably with the increase of the ORC evaporation temperature.
- The exergetic efficiency of the combined system increases significantly with the increase of CRS refrigeration temperature.
- The energy efficiency of the combined system increases considerably over the temperature range considered and reaches a maximum value of 75.15% at -30°C and the minimum value is 32.36% at -60°C of temperature.
- The exergy efficiency of the combined system decreases significantly with the increase of the ORC evaporation temperature.

NOMENCLATURE

\dot{E}_x	Exergy rate, kW
h	specific enthalpy, kJ/kg
\dot{m}	Masse flow rate, kg/s
P	Pressure, bar
\dot{Q}	Heat rate, kW
\dot{S}	Entropy generation, kW/K
s	Specific entropy, kJ/kg.K
T	Temperature, °C
\dot{W}	Mechanical Power, kW

Greek letters

η	Efficiency
--------	------------

Subscripts

C	Compressor
Cond	Condenser
Evap	Evaporator
Ev	Expansion valve
HEX	Heat exchanger
in	Input
out	Output
P	Pump
T	Turbine

Abbreviations

COP	Coefficient of performance
CRS	Compression Refrigeration System
ORC	Organic Rankine Cycle

ACKNOWLEDGEMENT

The authors thank the University Djilali Bounaama Khemis Miliana (Algeria) for funding this study.

AUTHORSHIP CONTRIBUTIONS

Concept: T.R.; Design: T.R.; Supervision: T.R., H.K.; Materials: T.R., H.K.; B.F., S.S.; Data: T.R., H.K.; Analysis: T.R., B.F., S.S.; Literature search: T.R., H.K., M.H.; Writing: T.R.; Critical revision: M.H., H.K

DATA AVAILABILITY STATEMENT

No new data were created in this study. The published publication includes all graphics collected or developed during the study.

CONFLICT OF INTEREST

The author declared no potential conflicts of interest with respect to the research, authorship, and/or publication of this article.

ETHICS

There are no ethical issues with the publication of this manuscript.

REFERENCES

- [1] Braimakis, K., & Karellas, S. Energetic optimization of regenerative Organic Rankine Cycle (ORC) configurations. *Energy Conversion and Management* 2018;159:353–370. <https://doi.org/10.1016/j.enconman.2017.12.093>.
- [2] Bellos, E., Vellios, L., Theodosiou, I. C., & Tzivanidis, C. Investigation of a solar-biomass polygeneration system. *Energy conversion and management* 2018;173:283–295. <https://doi.org/10.1016/j.enconman.2018.07.093>.
- [3] Bellos, E., & Tzivanidis, C. Parametric analysis and optimization of a solar driven trigeneration system based on ORC and absorption heat pump. *Journal of cleaner production* 2017;161:493–509. <https://doi.org/10.1016/j.jclepro.2017.05.159>.
- [4] Bellos, E., & Tzivanidis, C. Multi-objective optimization of a solar driven trigeneration system. *Energy* 2018;149:47–62. doi: 10.1016/j.energy.2018.02.054. Haut du formulaire
- [5] Li, T., Yuan, Z., Xu, P., & Zhu, J. Entransy dissipation/loss-based optimization of two-stage organic Rankine cycle (TSORC) with R245fa for geothermal power generation. *Science China Technological Sciences* 2016;59(10): 1524–1536. <https://doi.org/10.1007/s11431-016-0151-1>.

- [6] Guo, T., Wang, H., & Zhang, S. Comparative analysis of CO₂-based transcritical Rankine cycle and HFC245fa-based subcritical organic Rankine cycle using low-temperature geothermal source. *Science China Technological Sciences* 2010;53(6): 1638–1646. <https://doi.org/10.1007/s11431-010-3123-4>.
- [7] Heberle, F., & Brüggemann, D. Exergy based fluid selection for a geothermal Organic Rankine Cycle for combined heat and power generation. *Applied Thermal Engineering* 2010;30(11–12):1326–1332. <https://doi.org/10.1016/j.applthermaleng.2010.02.012>.
- [8] Liu, Q., Duan, Y., & Yang, Z. Performance analyses of geothermal organic Rankine cycles with selected hydrocarbon working fluids. *Energy* 2013;63: 123–132. <https://doi.org/10.1016/j.energy.2013.10.035>
- [9] Roy, D., & Ghosh, S. Energy and exergy analyses of an integrated biomass gasification combined cycle employing solid oxide fuel cell and organic Rankine cycle. *Clean Technologies and Environmental Policy* 2017;19(6):1693–1709.
- [10] Taljan, G., Verbič, G., Pantoš, M., Sakulin, M., & Fickert, L. Optimal sizing of biomass-fired Organic Rankine Cycle CHP system with heat storage. *Renewable Energy* 2012;41:29–38. <https://doi.org/10.1016/j.renene.2011.09.034>.
- [11] Gutiérrez-Arriaga, C. G., Abdelhady, F., Bamufleh, H. S., Serna-González, M., El-Halwagi, M. M., & Ponce-Ortega, J. M. Industrial waste heat recovery and cogeneration involving organic Rankine cycles. *Clean Technologies and Environmental Policy* 2015;17(3):767–779. <https://doi.org/10.1007/s10098-014-0833-5>.
- [12] Sun, W., Yue, X., & Wang, Y. Exergy efficiency analysis of ORC (Organic Rankine Cycle) and ORC-based combined cycles driven by low-temperature waste heat. *Energy Conversion and Management* 2017;135:63–73. <https://doi.org/10.1016/j.enconman.2016.12.042>.
- [13] Shaaban, S. Analysis of an integrated solar combined cycle with steam and organic Rankine cycles as bottoming cycles. *Energy conversion and management* 2016;126:1003–1012. <https://doi.org/10.1016/j.enconman.2016.08.075>.
- [14] Acar, M. S., & Arslan, O. Energy and exergy analysis of solar energy-integrated, geothermal energy-powered Organic Rankine Cycle. *Journal of Thermal Analysis and Calorimetry* 2019;137(2): 659–666.
- [15] Touaibi, R., Köten, H., Feidt, M., & Boydak, O. Investigation of three Organic Fluids Effects on Exergy Analysis of a Combined Cycle: Organic Rankine Cycle/Vapor Compression Refrigeration. *Journal of Advanced Research in Fluid Mechanics and Thermal Sciences* 2018;52(2):232–245.
- [16] Bu, X., Wang, L., & Li, H. Performance analysis and working fluid selection for geothermal energy-powered organic Rankine-vapor compression air conditioning. *Geothermal Energy* 2013;1(1): 2. <https://doi.org/10.1186/2195-9706-1-2>.
- [17] Saleh, B. Parametric and working fluid analysis of a combined organic Rankine-vapor compression refrigeration system activated by low-grade thermal energy. *Journal of advanced research* 2016;7(5):651–660. <https://doi.org/10.1016/j.jare.2016.06.006>.
- [18] Özdemir, e., & Milic, M. Thermodynamic analysis of basic and regenerative organic Rankine cycles using dry fluids from waste heat recovery. *Journal of thermal engineering* 2018;4(5):2381–2393. <http://doi.org/10.18186/thermal.439288>.
- [19] Kerme, E., & Orfi, J. Exergy-based thermodynamic analysis of solar driven organic Rankine cycle. *Journal of Thermal Engineering* 2015, 1(5):192–202.
- [20] Koroglu, T., & Oguz, S. Advanced exergy analysis of an organic Rankine cycle waste heat recovery system of a marine power plant. *Journal of Thermal Engineering* 2017;3(2):1136–1148. <https://doi.org/10.18186/thermal.298614>.
- [21] Touaibi, R., Feidt, M., Vasilescu, E. E., & Abbes, M. T. Modelling and Optimization Study of an Absorption Cooling Machine using Lagrange Method to Minimize the Thermal Energy Consumption. *Journal of Advanced Research in Fluid Mechanics and Thermal Sciences* 2019;58 (2): 207–218.
- [22] Touaibi, R., Feidt, M., Vasilescu, E. E., & Abbes, M. T. Parametric study and exergy analysis of solar water-lithium bromide absorption cooling system. *International Journal of Exergy* 2013;13(3):409–429.
- [23] Kalla, S. K., Arora, B. B., & Usmani, J. A. Performance analysis of R22 and its substitutes in air conditioners. *Journal of Thermal Engineering* 2018;4(1): 1724–1736. <https://doi.org/10.18186/journal-of-thermal-engineering.367419>.
- [24] Kutlu, Ç., Ünal, Ş., & Erdinç, M. T. Thermodynamic analysis of bi-evaporator ejector refrigeration cycle using R744 as natural refrigerant. *Journal of Thermal Engineering* 2016;2(2): 735–740. <https://doi.org/10.18186/journal-of-thermal-engineering.408659>.
- [25] Seckin, c. Investigation of the effect of the primary nozzle throat diameter on the evaporator performance of an ejector expansion refrigeration cycle. *Journal of thermal engineering* 2018;4(3): 1939–1953. <https://doi.org/10.18186/journal-of-thermal-engineering.408659>.
- [26] Lee, T. S., Liu, C. H., & Chen, T. W. Thermodynamic analysis of optimal condensing temperature of cascade-condenser in cascade refrigeration

- systems. *International Journal of Refrigeration* 2006; 29(7):1100–1108. <https://doi.org/10.1016/j.ijrefrig.2006.03.003>.
- [27] Getu, H. M., & Bansal, P. K. Thermodynamic analysis of an R744–R717 cascade refrigeration system. *International journal of refrigeration* 2008; 31(1):45–54. <https://doi.org/10.1016/j.ijrefrig.2007.06.014>.
- [28] Kilicarslan, A., & Hosoz, M. Energy and irreversibility analysis of a cascade refrigeration system for various refrigerant couples. *Energy Conversion and Management* 2010;51(12):2947–2954. <https://doi.org/10.1016/j.enconman.2010.06.037>.
- [29] Dopazo, J. A., Fernández-Seara, J., Sieres, J., & Uhía, F. J. Theoretical analysis of a cascade refrigeration system for cooling applications at low temperatures. *Applied Thermal Engineering* 2009;29(8–9):1577–1583. <https://doi.org/10.1016/j.applthermaleng.2008.07.006>.
- [30] Dopazo, J. A., & Fernández-Seara, J. Experimental evaluation of a cascade refrigeration system prototype with CO₂ and NH₃ for freezing process applications. *International Journal of Refrigeration* 2011, 34(1):257–267. <https://doi.org/10.1016/j.ijrefrig.2010.07.010>.
- [31] Ust, Y., & Karakurt, A. S. Analysis of a Cascade Refrigeration System (CRS) by Using Different Refrigerant Couples Based on the Exergetic Performance Coefficient (EPC) Criterion. *Arabian Journal for Science and Engineering* 2014;39(11):8147–8156. <https://doi.org/10.1007/s13369-014-1335-9>.
- [32] Yun, E., Park, H., Yoon, S. Y., & Kim, K. C. Dual parallel organic Rankine cycle (ORC) system for high efficiency waste heat recovery in marine application. *Journal of Mechanical Science and Technology* 2015;29(6):2509–2515. <http://dx.doi.org/10.1007/s12206-015-0548-5>.
- [33] Molés, F., Navarro-Esbrí, J., Peris, B., Mota-Babiloni, A., & Kontomaris, K. K. Thermodynamic analysis of a combined organic Rankine cycle and vapor compression cycle system activated with low temperature heat sources using low GWP fluids. *Applied Thermal Engineering* 2015;87:444–453. <https://doi.org/10.1016/j.applthermaleng.2015.04.083>.
- [34] Sadreddini, A., Ashjari, M. A., Fani, M., & Mohammadi, A. Thermodynamic analysis of a new cascade ORC and transcritical CO₂ cycle to recover energy from medium temperature heat source and liquefied natural gas. *Energy Conversion and Management* 2018;167:9–20. <https://doi.org/10.1016/j.enconman.2018.04.093>.
- [35] Lizarte, R., Palacios-Lorenzo, M. E., & Marcos, J. D. Parametric study of a novel organic Rankine cycle combined with a cascade refrigeration cycle (ORC-CRS) using natural refrigerants. *Applied Thermal Engineering* 2017;127:378–389. <https://doi.org/10.1016/j.applthermaleng.2017.08.063>.
- [36] Yilmaz, F., Ozturk, M., & Selbas, R. Energy and exergy performance assessment of a novel solar-based integrated system with hydrogen production. *International journal of hydrogen energy* 2019; 44(34):18732–18743. <https://doi.org/10.1016/j.ijhydene.2018.10.118>.
- [37] Ishaq, H., Dincer, I., & Naterer, G. F. Exergy-based thermal management of a steelmaking process linked with a multi-generation power and desalination system. *Energy* 2018;159:1206–1217. <https://doi.org/10.1016/j.energy.2018.06.213>.